Damping characteristics of cable stayed bridges

K. Kawashima & S. Unjoh

Public Works Research Institute, Ministry of Construction, Tsukuba Science City, Japan

ABSTRACT : Seismic behavior of cable stayed bridges is presented with emphasis on damping characteristics. Dependence of damping ratio on mode shapes through free oscillation tests of a cable stayed bridge model is presented. A method to evaluate damping ratio of a total bridge system is proposed.

1 INTRODUCTION

Cable stayed bridges have not yet experienced significant earthquakes in the past. According to the previous field forced vibration tests on cable stayed bridges, it is well recognized that the natural frequencies and the natural mode shapes measured from the experiments can be predicted with satisfactory accuracy by appropriate analytical simulations[1]. However, in many cases damping ratios determined from the field forced excitation tests conducted in the past are likely to show considerably smaller value compared to the values assumed in seismic design. Because the structural response of cable stayed bridges significantly depends on the damping ratio, correct estimation of the damping ratio is of critical importance in seismic design.

It is the objectives of this paper to discuss damping characteristics of cable stayed bridges. Cable configuration dependence of damping ratio through model oscillation tests is presented. A method to predict damping ratio of cable stayed bridges is proposed. Engineering significance of the damping ratio is studied placing emphasis on how the damping ratio depends on mode shapes and amplitude.

2 Experimental Model and Free Oscillation Tests

To study damping characteristics of cable stayed bridges, a series of model oscillation tests were made. Fig.1 shows an experimental model which was accurately fabricated for simulating the Meiko-nishi Bridge as prototype. The rigidity and mass of the model was determined assuming the scale of length, density and time of 1/150, 1/1 and $1/\sqrt{150}$, respectively.

The deck was supported by only cables so that friction between the deck and the tower due to relative movement of the deck in longitudinal direction can be disregarded. The elastic cable restrainers was disregarded in the model for simplicity. Cable arrangement and number of cables were varied as 3 cases as shown in Fig.2. Fig.3 shows the fundamental natural frequencies and natural mode shapes of the model predicted by a linear discrete frame model.
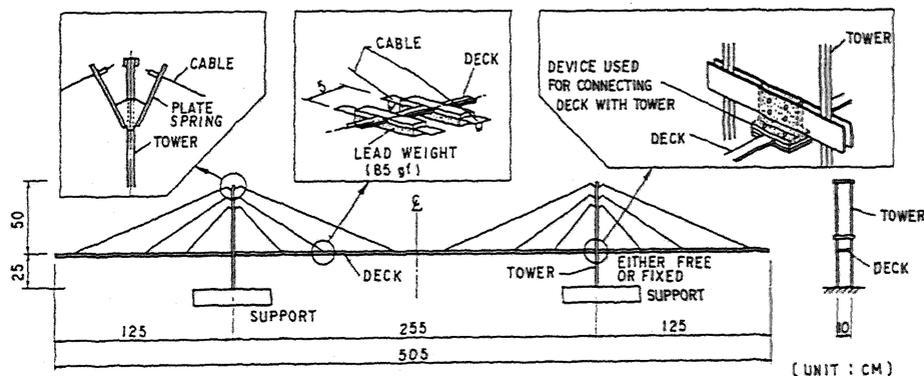

Fig.1 Experimental Bridge Model

The deck was statically displaced so as to create an initial deformation close to the target mode shape. It was smoothly released to result in a free oscillation. Damping ratio was computed from decay of free oscillation as

$$\delta = \frac{2\pi h}{\sqrt{1 - h^2}} = \log_e \frac{a_m}{a_{m+1}} \quad (1)$$

in which δ and h represent logarithmic damping ratio and damping ratio of critical, respectively, and a_m and a_{m+1} represent amplitude of free oscillation at m-th and (m+1)th oscillation, respectively.

Cable type dependence of the damping ratio is considerable as shown in **Fig.4(a)**. The damping ratio at the same amplitude increases as the cable type changes from the fan type (Type 3A) to the harp type (Type 3E). Such a significant cable type dependence of the damping ratio may be clearly related with the flexural deformation of the deck in vertical direction per unit deck displacement in longitudinal direction as shown in **Fig.3**. Larger flexural deformation of the deck in vertical direction dissipates larger energy, which would result in larger damping ratio.

The damping ratio also depends on the amplitude, and its amplitude dependence increases as the cable type changes from the fan type(Type 3A) to the harp type (Type 3E). The amplitude dependence of the damping ratio tends to increase as the amplitude becomes smaller.

Damping ratio decreases as the cable type changes from the fan type (Type 3A) to the harp type (Type 3E) as shown in **Fig.4(b)**. Damping ratio for the flexural oscillation in vertical direction is generally smaller than that for the longitudinal oscillation. However it is quite interesting to note that such cable type dependence of the damping ratio is opposite in order to that developed in the longitudinal oscillation.

3 EVALUATION METHOD OF DAMPING RATIO OF CABLE STAYED BRIDGES

There are various factors causing energy dissipation in cable stayed bridges. Energy dissipation is generally developed by material nonlinearity, structural damping such as friction at movable bearings, radiation of energy from foundations to subground, and friction with air. Predominant factors contributing to damping ratio of cable stayed bridges vary with structural types. However important point to estimate damping ratio of cable stayed bridges is to evaluate total energy dissipation.
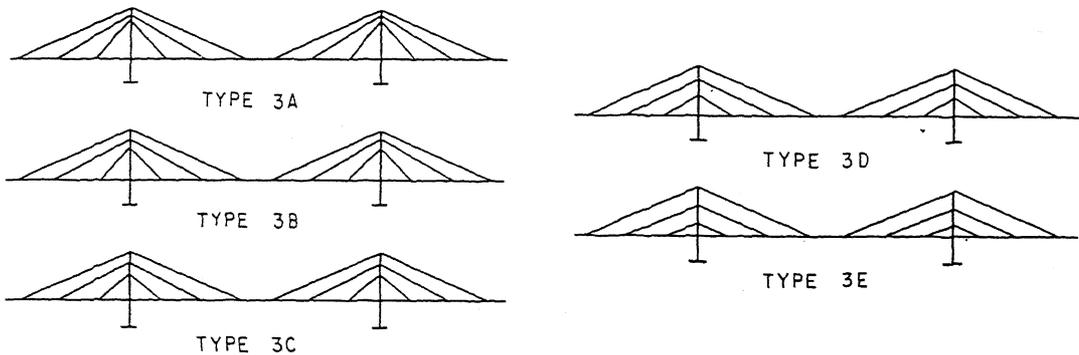
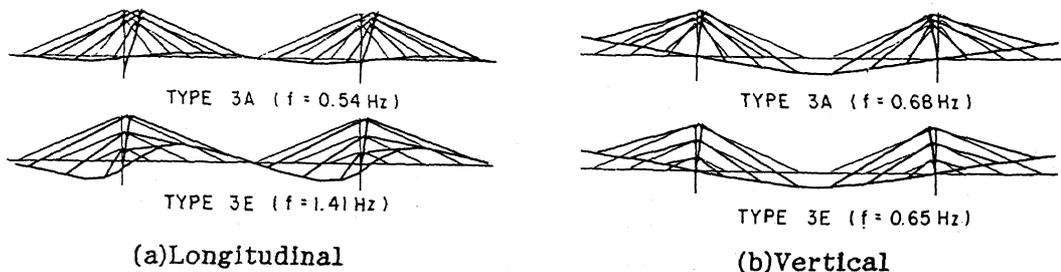Fig.2 **Cable Arrangement of Bridge Model**

(a)Longitudinal

(b)Vertical

Fig.3 **Predicted Mode Shapes**

(a) Longitudinal Oscillation
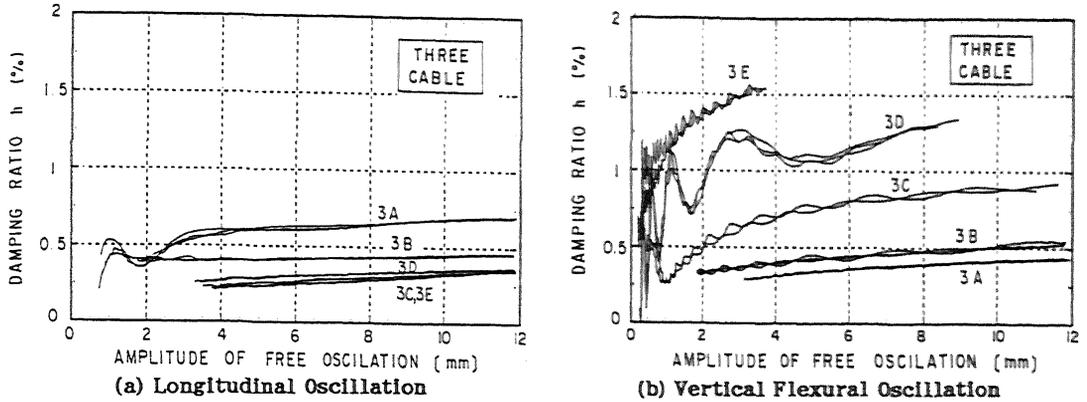

(b) Vertical Flexural Oscillation

Fig.4 Damping Ratio vs. Oscillation Amplitude

Because the energy dissipation capability may not be the same in the whole bridge, it is required to evaluate the energy dissipation in each structural segment depending on the type of the energy dissipation. Once the energy dissipation in individual structural segments can be determined, the total energy dissipation in the whole structural system may be evaluated by summing up the energy dissipation developed in each structural segment.

Based on such considerations, it is proposed to evaluate energy dissipation of a cable stayed bridge as;

1) Divide a cable stayed bridge into several structural segments in which energy dissipation capability can be considered practically the same. Such a structural segment is referred hereinafter as "sub-structure".

2) When the i-th sub-structure is idealized by a n-degree of freedom discrete system, the strain energy $E_J{}^i$ of the i-th sub-structure for j-th mode may be represented as

$$E_J{}^i = \frac{1}{2} \sum_k (u_J{}^{ik})^T k^i u_J{}^{ik} \qquad (2)$$

in which $u_J{}^{ik}$ = amplitude at node k of i-th sub-structure for j-th mode and k^i = stiffness matrix of the i-th sub-structure.

Strain energy of the whole structural system for j-th mode can, then, be evaluated as

$$E_J = \sum_i E_J{}^i \qquad (3)$$

3) For the i-th sub-structure where energy dissipation due to material nonlinearity is predominant, the energy dissipation associated with j-th mode may be written as

$$\delta E_J{}^i = f_J{}^i(E_J{}^i) \qquad (4)$$

in which $\delta E_J{}^i$ = energy dissipation in i-th

sub-structure for j-th mode, $E_J{}^i$ = strain energy in i-th sub-structure for j-th mode, and $f_J{}^i$ = function relating $\delta E_J{}^i$ with $E_J{}^i$.

The function $f_J{}^i$ represents how the energy dissipation in i-th substructure $\delta E_J{}^i$ be developed associated with the strain energy in i-th sub-structure $E_J{}^i$. This is referred hereinafter as "energy dissipation function". Because it is quite difficult in most cases to directly evaluate the energy dissipation function $f_J{}^i$ from analytical studies, it has to be determined based on appropriate experiments.

4) For i-th sub-structure where the energy dissipation function $f_J{}^i$ is such a form that it can be represented in terms of a displacement at a specific point $u_J{}^{ik}$ within the i-th sub-structure, the energy dissipation function may be represented as

$$\delta E_J{}^i = f_J{}^i(u_J{}^{ik}) \qquad (5)$$

in which $\delta E_J{}^i$ = energy dissipation in i-th sub-structure for j-th mode, $u_J{}^{ik}$ = displacement at point k in i-th sub-structure for j-th mode, and $f_J{}^i$ = energy dissipation function relating $\delta E_J{}^i$ with $u_J{}^{ik}$.

5) Energy dissipation in the whole structural system can be obtained by summing up the energy dissipation developed in individual sub-structures determined by Eqs.(4) and/or (5) as

$$\delta E_J = \sum_i \delta E_J{}^i \qquad (6)$$

in which δE_J = total energy dissipation in whole structure for j-th mode, and $\delta E_J{}^i$ = energy dissipation in i-th sub-structure for j-th mode.

6) Damping ratio of the whole structure for j-th mode may then be obtained from Eqs.(3) and (6) as

$$h_J = \frac{\delta E_J}{4 \pi E_J} \qquad (7)$$

4 Evaluation of Energy Dissipation Functions

To show an evaluation of the energy dissipation functions, it is appropriate to refer a specific bridge for which actual damping characteristics was accurately estimated. Therefore, the energy dissipation functions are evaluated for the cable stayed bridge model presented in the preceding section.

Because the model bridge was supported by only cables, friction between the deck and the tower can be neglected. Effect of radiation of energy from the foundation to subsoils can be neglected in the model because bottom of the tower was rigidly fixed by a steel base plate. Therefore it was assumed that the energy dissipation of the model bridge occurs due to material nonlinearity of the deck and the tower, and friction at the anchoring portion of the cables to the deck and the tower. The tower, the deck and the cable anchoring portion were therefore considered as "substructure" in the analysis.

For estimating the energy dissipation function of the tower, a simple free oscillation test of the tower was made as shown in **Fig.5**. Only the tower was taken out from the whole model, and it was supported as a cantilevered beam with one of the ends being fixed and the other being free. By smoothly releasing the tower top from a displaced position, a free oscillation simulating the first mode was developed.

Fig.6 shows how the damping ratio of the tower varies with the oscillation amplitude and the mass of the weight placed on the free end. Predicted damping ratio which will be described later is also presented for comparison. Damping ratio of the tower increases as the oscillation amplitude increases.

Because the damping ratio h_1 of the tower for the first mode shape can be determined through the decay of the free oscillation and the strain energy E_1 can be computed from Eq.(2), one can determine the energy dissipation δE_1 by substituting h_1 and E_1 into Eq.(7).

Fig.7 shows the relation between δE_1 and E_1 for the first mode. The relation seems almost independent of the weight of the mass placed on the tower top. It was approximated by a least square fit as

$$\delta E_1 = 0.016 E_1 + 0.0021 E_1^{3/2} \qquad (8)$$

Based on Eq.(8), the damping ratio vs. the oscillation amplitude of the tower was evaluated as shown in **Fig.6**. It is seen that the predicted damping ratio for the tower agrees reasonably well with the experimental result.

The energy dissipation functions for the deck and the connection between cables and towers and between cables and deck (cable anchoring portion) were similarly evaluated

from **Figs.8~11** as

$$\delta E_1 = 0.016 E_1 + 0.083 E_1^{1.37} \quad \text{(deck)} \qquad (9)$$

$$\delta E_1 = 0.018 \omega^{2.15} \cdot \theta^2 \quad \text{(cable anchoring portion)} \qquad (10)$$

in which θ and ω represent an angle between the tower and the cable, and angular frequency of the free oscillation, respectively. The cable anchoring portion is an important place where large amount of energy is dissipated.
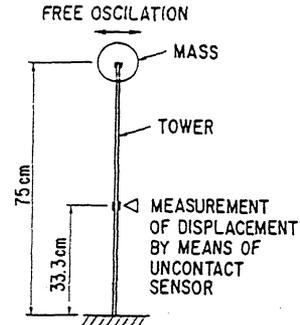

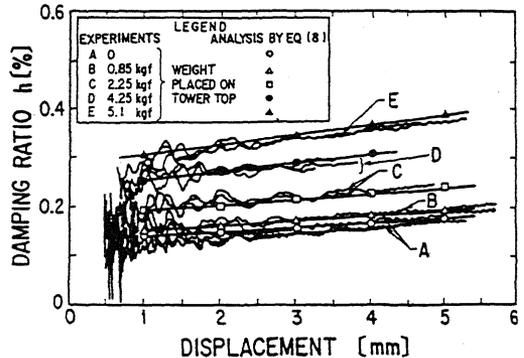**Fig.5 Free Oscillation Test for Tower**

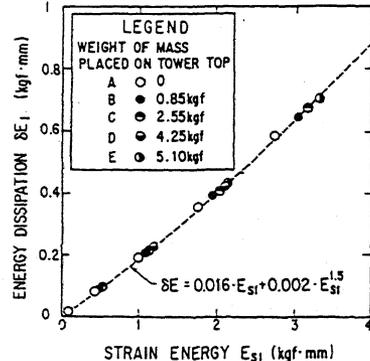**Fig.6 Damping Ratio vs. Oscillation Amplitude for Tower**

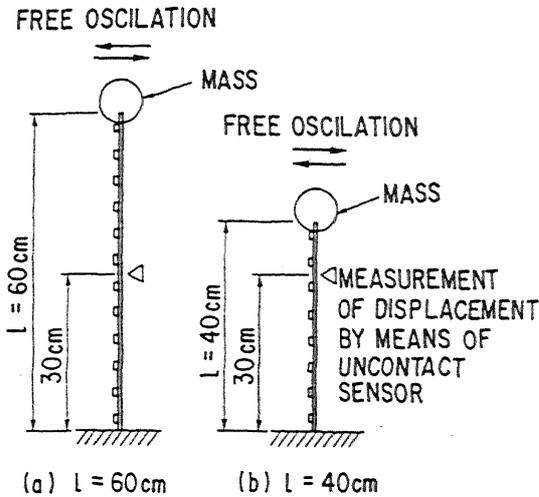**Fig.7 Energy Dissipation δE_1 vs. Strain Energy E_1 for Tower (1 kgf = 9.81 N)**
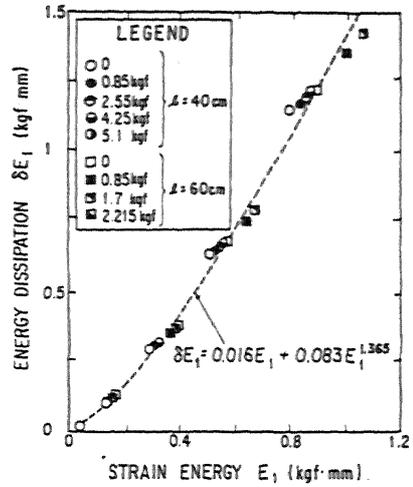
FREE OSCILATION

MASS

FREE OSCILATION

MASS

$l = 60$ cm
30cm

$l = 40$ cm
30cm

◁MEASUREMENT
OF DISPLACEMENT
BY MEANS OF
UNCONTACT
SENSOR

(a) $l = 60$ cm   (b) $l = 40$ cm

Fig.8 Free Oscillation Test for Deck

Fig.9 Energy Dissipation δ E₁ vs. Strain Energy E₀₁ for Deck (1 kgf = 9.81 N)

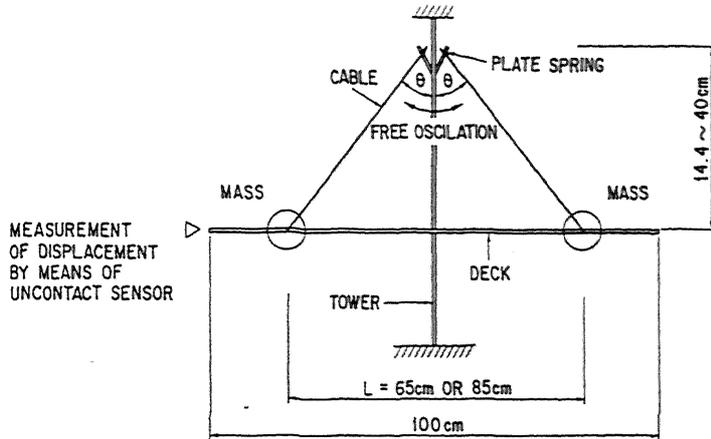$\delta E_1 = 0.016 E_1 + 0.083 E_1^{1.365}$

Fig.10 Free Oscillation Test for Anchoring Portion
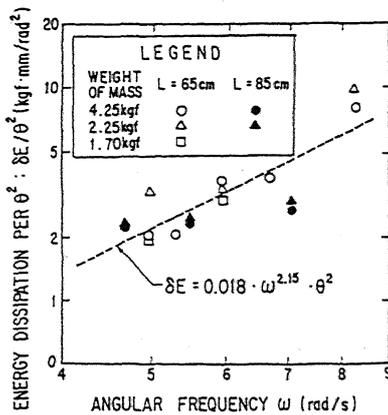
Fig.11   Energy   Dissipation,   Angular Frequency and   Free Oscillation Test for Anchoring Portion

$\delta E = 0.018 \cdot \omega^{2.15} \cdot \theta^2$

5 Evaluation of Damping Ratio Based on Energy Dissipation Functions

Predicted damping ratio by Eq.(7) assuming the energy dissipation functions of the sub-structures by Eqs.(8), (9) and (10) is presented in **Fig.8** in comparison with the experimental results.

The predicted damping ratio of the model in the longitudinal oscillation increases as the cable type changes from the fan type (type 3A) to the harp type (type 3E) in the same manner with the test. The dependence of the predicted damping ratio on the oscillation amplitude increases in the same order with the experiments. Such characteristics agree reasonably well with the experiments, although the predicted damping ratio is underestimated as the cable type approaches to the harp type.

The predicted damping ratio of the model for the vertical flexural oscillation is almost independent of the cable type. Although the damping ratio estimated from the experiments slightly decreases as the cable type changes from the fan type to the harp type, the overall characteristics of the predicted damping ratio seem reasonably close with the experimental results.

The damping ratio predicted is somewhat smaller than the experimental results probably because the energy dissipation which are not considered in this analysis would contribute to the total energy dissipation. If the energy dissipation at each portion is evaluated in detail, it is expected that the accuracy of the above estimation be further improved.
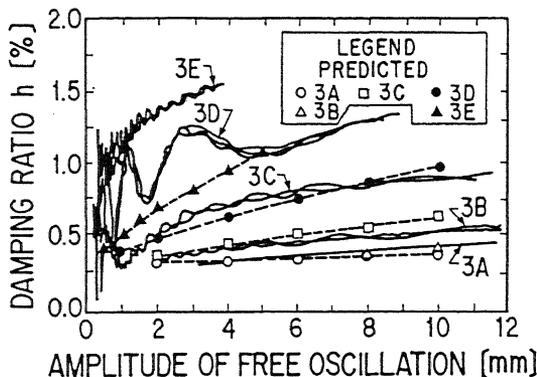
(a) Longitudinal Oscillation
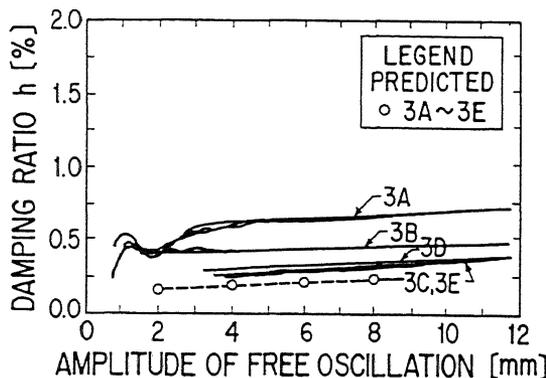
(b) Flexural Vertical Oscillation

Fig.8 Prediction of Damping Ratio vs. Oscillation Amplitude Relation

6 CONCLUDING REMARKS

Cable stayed bridges have complex dynamic behavior, and it is of great importance to correctly evaluate their dynamic characteristics for developing a rational seismic design method. The characteristics of damping which were presented in the preceding pages may be summarized as :

1) Damping ratio depends on the mechanism of energy dissipation and the mode shapes. It is therefore important to consider what type of and how much energy dissipation are made in each sub-structure. Even in the same bridge, different damping ratio may be measured if the direction or the point of excitation is different because of the difference of the mode shapes considered. Unless taking considerations on such characteristics into account, attempts to formulate empirical relations for assessing the damping ratio would only cause large scatters around the prediction.

2) Dependence of the damping ratio on the mode shape seems to be one of the reasons which cause considerable scatters observed in the past forced excitation tests results.

3) Cable configuration such as number of cables and type of cable arrangement is a controlling factor for damping ratio. The harp type cable arrangement tends to develop larger damping ratio than the fan type cable arrangement for the oscillation mode in longitudinal direction, because it causes larger deck deformation in vertical direction.

4) Application of the proposed method for assessing the damping ratio of cable stayed bridges needs to be made. It is required to conduct careful and elaborate forced excitation tests so that the energy dissipation mechanism in sub-structures can be clarified.

REFERENCES

Kawashima, K., Unjoh, S. and Tsunomoto, M. : Damping Characteristics of Cable Stayed Bridges for Seismic Design, Journal of Research, Vol.27, Public Works Research Institute, December 1991

Kawashima, K., Unjoh, S. and Azuta, Y. : Analysis of Damping Characteristics of A Cable Stayed Bridge Based on Strong Motion Records, Proc. Japan Society of Civil Engineers, Structural Eng./Earthquake Eng., Vol.7, No.1, April 1990, pp.181-190

Narita, N. : Forced Vibration Test of Suigo Bridge, Technical Note, Vol. 1349, Public Works research Institute, 1978

Kawashima, K. and Unjoh, S. : Damping Characteristics of Cable Stayed Bridges Associated with Energy Dissipation at Movable Supports, Proc. Japan Society of Civil Engineers, Structural Eng./ Earthquake Eng., Vol.6, No.1, April 1989, pp.145-152

Kawashima, K., Unjoh, S. and Azuta, Y. : Damping Characteristics of Cable Stayed Bridges, Proc. 9th World Conference on Earthquake Engineering, Tokyo/Kyoto, Japan, August 1988